

EFFICIENT CONTAMINANT REMOVAL FROM LIQUID DIGESTATE OF PIG MANURE BY CHEMICAL PRECIPITATION AND CO₂ MINERALIZATION USING ALKALINE ASH

Zhengxin FEI (✉)¹, Zijie DING², Xuan ZHENG², Liang FENG², Qingyao HE², Shuiping YAN², Long JI (✉)²

¹ College of Pharmaceutics, Jinhua Polytechnic, Jinhua 321007, China.

² Technology & Equipment Center for Carbon Neutrality in Agriculture, College of Engineering, Huazhong Agricultural University, Wuhan 430070, China.

KEYWORDS

anaerobic digestion, chemical oxygen demand, fly ash, ion removal, total phosphate

HIGHLIGHTS

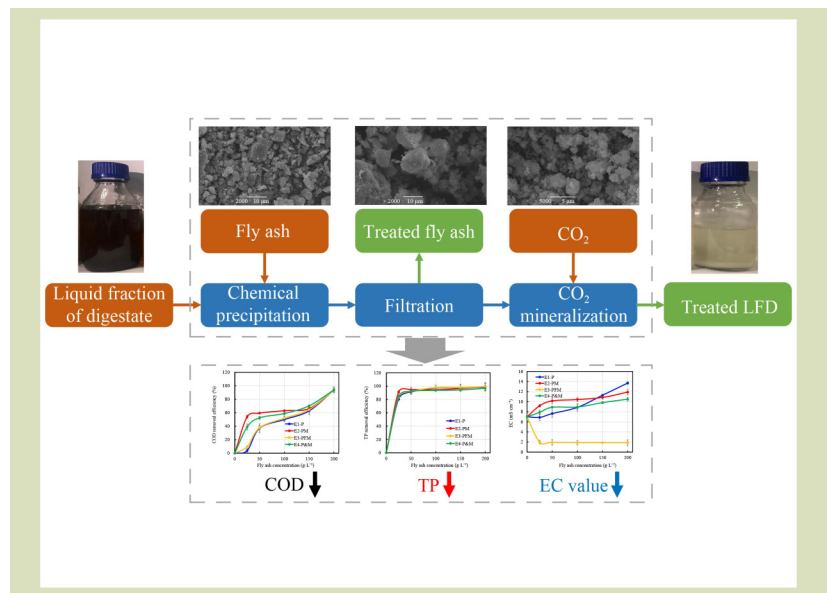
- LFD was treated by fly ash-based chemical precipitation and CO₂ mineralization.
- > 93% COD and > 98% TP removal efficiency, and < 2 mS·cm⁻¹ EC was achieved.
- COD and TP removal was achieved by co-precipitation during CO₂ mineralization.
- CO₂ mineralization neutralized the alkaline LFD and removed heavy met.

Received August 8, 2022;

Accepted December 19, 2022.

Correspondences: 20050910@jhc.edu.cn,
long.ji@mail.hzau.edu.cn

GRAPHICAL ABSTRACT



ABSTRACT

Chemical precipitation is a widely applied approach for a liquid fraction of digestate (LFD) of agricultural waste but its large-scale application requires low-cost and efficient precipitating agents and novel process design. This study evaluated novel approach for the efficient removal of contaminants from the LFD using fly ash-based chemical precipitation, followed by filtration and CO₂ mineralization. The technical feasibility of this approach was evaluated using pH and electrical conductivity (EC), and removal efficiencies of total phosphorus (TP), chemical oxygen demand (COD) and heavy metals during the treatment. The fly ash used in this study showed a promising performance as a chemical precipitation agent for COD and TP removal from the treated LFD involving complex effects of precipitation and adsorption. CO₂ bubbling after fly ash-based chemical precipitation provided further COD and TP removal by

carbonation reactions between CO₂ and the excessive alkaline minerals in fly ash. Although addition of fly ash to untreated LFD increased pH from 8.3 to 12.9 and EC from 7.01 to 13.7 mS·cm⁻¹, CO₂ bubbling helped neutralize the treated LFD and reduce the EC, and concentrations of toxic ions by carbonation reactions. The fly ash-based chemical precipitation and CO₂ mineralization had > 93% COD and > 98% TP removal efficiencies, and resulted in an EC of < 2 mS·cm⁻¹ and a neutral pH in the treated LFD, as well as the high purity calcite product.

© The Author(s) 2023. Published by Higher Education Press. This is an open access article under the CC BY license (<http://creativecommons.org/licenses/by/4.0>)

1 INTRODUCTION

Anaerobic digestion is a promising technology to deal with the increasing volume of global agricultural waste^[1]. It takes advantage of biogas generation, process stability and low operating costs. However, the liquid fraction of digestate (LFD) discharged from the anaerobic plants has high chemical oxygen demand (COD) and contains high phosphate concentration^[2,3]. The discharge of LFD without proper treatment may lead to environmental risks, such as the eutrophication of water bodies^[4]. Therefore, contaminant removal from the LFD before discharge is a matter of great concern. LFD is widely used as an organic fertilizer given its high nutrient content can increase crop yields and reduce the need for mineral fertilizer application^[5,6]. However, the direct application of LFD as a fertilizer is always restricted by the growing season and the area of available farmland^[4]. Also, the continuous application of LFD to farmland can result in serious leaching of nutrient from the soil to water bodies^[1]. In addition, the potential risk of toxic metals accumulation from LFD into crops is not clear.

Various alternative technologies for LFD treatment have been reported in the literature, including chemical precipitation^[7,8], flocculation-coagulation^[9], air stripping^[10], membrane separation^[11], ion exchange^[12], adsorption^[13], evaporation^[14], chemical oxidation or advanced oxidation, and microalgal cultivation^[15–17]. Chemical precipitation, as a widely applied pretreatment approach for wastewater treatment, aims to remove phosphate, heavy metals and organic contaminants^[8]. Compared to other LFD treatment technologies, chemical precipitation takes advantage of simple configurations and low capital costs. It is based on the reactions of metallic and nonmetallic ions to form insoluble precipitates which are then removed by filtration or sedimentation^[18]. Several chemical precipitating agents have been developed for LFD treatment, such as lime (CaO), hydrated lime (Ca(OH)₂) and magnesium oxide (MgO)^[19,20]. However, currently-

practiced chemical precipitation are limited by high operating costs because of the constant consumption of chemical agents and the treatment of sludge formed in the process. To improve the large-scale application of this technology, low-cost and efficient precipitating agents, and novel process designs will be essential.

Coal fly ash, a byproduct of coal combustion power plants, has been considered a promising precipitation agent for LFD treatment because of its high alkalinity and metal content, and particularly large volume production worldwide. The worldwide generation of coal fly ash was about 1.1 Gt in 2019^[21], although 53% of this is used for construction materials, the remainder sent to landfill^[22]. Considering the decreasing amount of landfill area available for fly ash disposal and increasing disposal cost, it is essential to develop new uses for fly ash. However, fly ash-based chemical precipitation of LFD is not widely reported in the literature^[18]. In addition, although chemical precipitation allows the simultaneous removal of several organic and inorganic contaminants, its use is still constrained by the extensive dissolution of alkaline minerals from the fly ash into the LFD, such as OH⁻, Ca²⁺, and Mg²⁺, which leads to the increased pH and electrical conductivity (EC) after treatment of LFD. The post-treated effluent must be neutralized and desalted to meet the pH and EC requirements for direct discharge. Also, toxic ions, especially heavy metals, are dissolved from the fly ash into the LFD during the treatment, which adds environmental risks for the further use of the treated LFD.

To deal with these challenges, this study evaluated a sustainable approach for LFD treatment by integrating fly ash-based chemical precipitation with CO₂ mineralization. CO₂ mineralization is a promising CO₂ capture and storage technology in which alkaline minerals react with CO₂ from the gas streams (e.g., flue gas and biogas) in the presence of water to form stable carbonates^[23]. CO₂ mineralization after fly ash-based chemical precipitation is not only expected to eliminate

the unwanted metal ions but also neutralize the excess alkalinity of the treated LFD. An earlier study indicated that CO₂ mineralization might induce additional removal of organic contaminants by co-precipitation with Ca²⁺ and CO₃²⁻ to form CaCO₃[24,25]. The organic contaminants with carboxyl, hydroxyl and other functional groups can adsorb multivalent cations by electrostatic interaction[26,27]. By bubbling CO₂ into LFD, the precipitation reaction of CaCO₃ can occur while organic contaminants can be gradually embedded in the precipitates[28,29] and removed from the treated LFD. Therefore, CO₂ mineralization has the potential to efficiently remove inorganic-organic contaminants from the treated LFD.

This study aimed to confirm the technical feasibility of this process and explore the underlying mechanism. A typical LFD was treated with fly ash-based to effect chemical precipitation, which was then followed by filtration and CO₂ mineralization. The pH and EC, and removal efficiencies of total phosphorus (TP), COD, and heavy metals during the treatment were measured. The physicochemical property of fly ash and LFD before and after the experiments was analyzed to determine the underlying mechanism.

2 MATERIALS AND METHODS

2.1 Materials

Fly ash was supplied by Huadian Electric Power Research Institute Co., Ltd., China. The elemental composition of the original fly ash sample was determined using X-ray fluorescence spectrometry and the results are given in Table 1. Crystalline phases of the unused fly ash were determined by X-ray diffractometry (XRD, D8 Advance Buker, Germany). Morphological investigation of the unused fly ash was performed with scanning electron microscopy (SEM, NTC JSM-6390LV, NTC, Japan).

LFD was collected from a mesophilic (~35 °C) anaerobic digestion plant located in Wuhan City, Hubei Province, China that has used pig manure as the substrate. The untreated LFD was stored anaerobically at ambient temperature before treatment until no more biogas was produced. The untreated LFD sample was characterized for its main physicochemical

Table 1 Elemental composition of fly ash samples (given as oxides)

Constituent	SiO ₂	Al ₂ O ₃	CaO	MgO	SO ₃	Fe ₂ O ₃	K ₂ O	Na ₂ O	P ₂ O ₅
Fraction (wt%)	30.2	29.3	21.5	0.7	9.6	4.7	0.7	0.4	0.3

properties. The pH was determined using a pH meter (FE28, Metler Toledo, Switzerland) and EC with a conductivity meter (DDS-307A, Shanghai INESA Scientific Instrument Co., Ltd., China). COD was measured using a COD meter (CM-03, Beijing Shuanghui Jingcheng Electronics Co., Ltd., China). CO₂ loading of the anaerobic digestate was tested by a standard acid titration method. Total ammonia nitrogen (TAN) concentration was determined in a Smartchem 200 Discrete Auto Analyzer (AMS-Westco, Italy). Heavy metal concentrations (As, Cd, Cr, Cu, Mn, Ni, Pb, and Zn) were determined by an Inductively Coupled Plasma Optical Emission Spectrometer (ICP-AES, 5110VDV, Agilent, United States). The characteristics of untreated LFD are shown in Table 2.

2.2 Contaminant removal experiments

Four experimental methods were evaluated for removal of contaminants from the untreated LFD (Fig. 1). All the experiments were run at room temperature with 250 mL of untreated LFD. The untreated LFD was placed into a glass bottle and continuously stirred at 200 r·min⁻¹ with a magnetic stirrer (DF-101-51, Zhengzhou Taiyuan Instrument Equipment Co., Ltd., China). The time that fly ash was added to the untreated LFD was recorded as the starting time of the chemical precipitation reaction. Five fly ash concentrations assessed were 25, 50, 100, 150 and 200 g·L⁻¹.

Experiment EI-P: Contaminant removal by fly ash-based chemical precipitation. For each experiment, 24 h was allowed for chemical precipitation then stirring was stopped and the suspension collected. The suspension was immediately filtered through a 0.20-μm filter unit equipped with a vacuum pump. The pH and EC of the filtrate were measured. The COD, TP, TAN and heavy metal concentrations of the filtrate were measured after microwave digestion. The filter cake was oven-dried overnight at 105 °C and then analyzed by XRD and SEM to determine the mineralogy and morphology properties.

Table 2 Characteristics of the untreated liquid fraction of digestate used in this study

Parameter	Value
pH	8.3
Electrical conductivity (mS·cm ⁻¹)	7.02
Chemical oxygen demand (mS·cm ⁻¹)	817
CO ₂ loading (mol·L ⁻¹)	0.061
Total phosphorous content (mg·L ⁻¹)	21.5

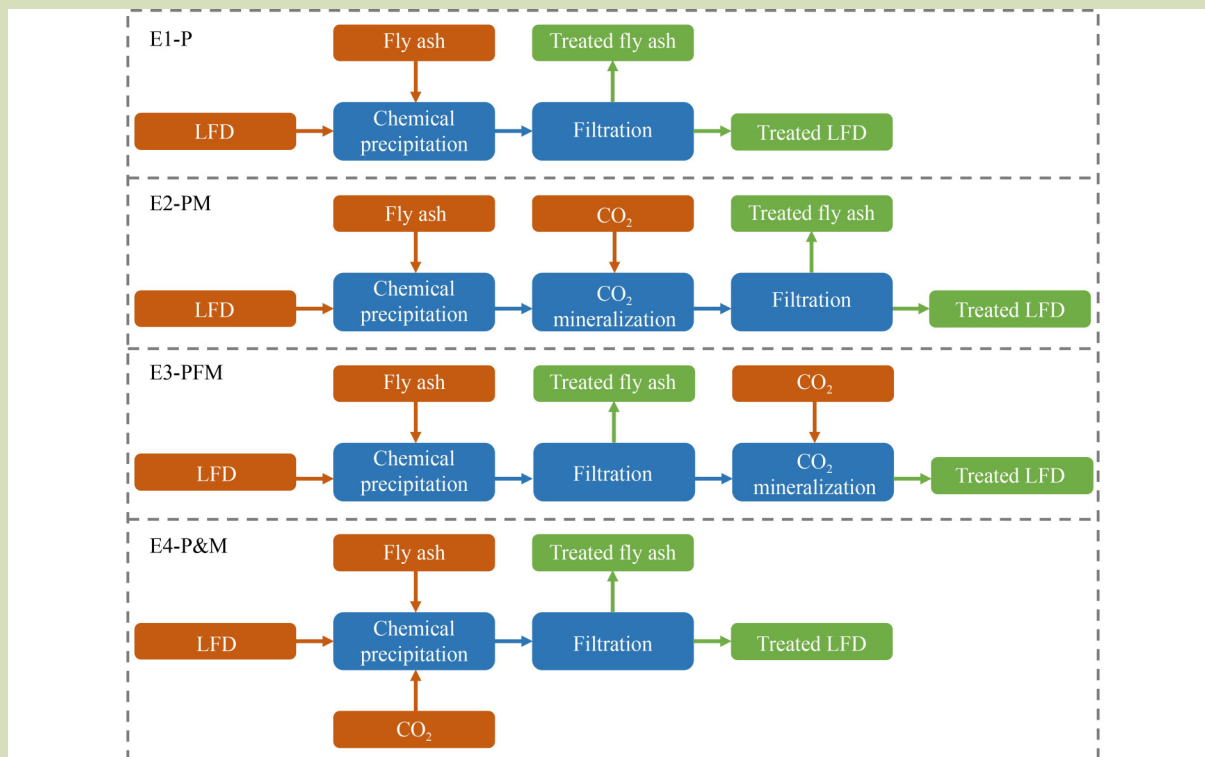


Fig. 1 Schematic indicating the processing steps for the four experiments used for liquid fraction of digestate (LFD) treatment.

Experiment E2-PM: Contaminant removal by fly ash-based chemical precipitation, followed by CO₂ mineralization. For each experiment, 24 h was allowed for chemical precipitation then CO₂ was bubbled into the suspension to promote CO₂ mineralization reactions. pH was measured every 5 min. After CO₂ bubbling for 40 min, stirring was stopped. The subsequent procedures were as experiment E1-P.

Experiment E3-PFM: Contaminant removal by fly ash-based chemical precipitation, followed by filtration and CO₂ mineralization of filtrate. For each experiment, 24 h was allowed for chemical precipitation then the suspension was immediately filtered through a 0.20-µm filter. CO₂ was bubbled into the filtrate to promote CO₂ mineralization reactions. pH was measured every 5 min. After CO₂ bubbling for 40 min, the stirring was stopped and the suspension was collected (Fig. 2). The subsequent procedures were as experiment E1-P.

Experiment E4-P&M: Contaminant removal by chemical precipitation and CO₂ mineralization in a single step. For each experiment, at the time of adding fly ash to the untreated LFD, CO₂ was also bubbled into the suspension to promote the chemical precipitation and CO₂ mineralization reactions. pH of the suspension was measured every 5 min. After CO₂

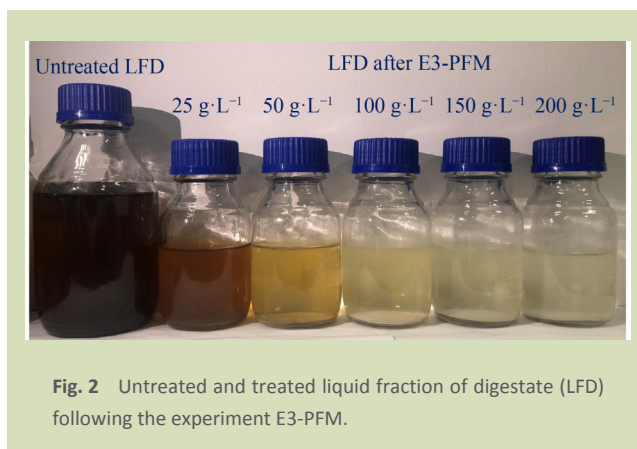


Fig. 2 Untreated and treated liquid fraction of digestate (LFD) following the experiment E3-PFM.

bubbling for 40 min, the stirring was stopped. The subsequent procedures were as experiment E1-P.

2.3 Leaching from fly ash

To investigate the amount of metallic components that leached from the used fly ash, the British Standard method (EN 12457-2) was applied. Used fly ash samples from experiments E1-P and E2-PM were mixed with ultrapure water at 100 g·L⁻¹. The suspension was stirred for 24 h at 200 r·min⁻¹ and then filtered

through a 0.20- μm filter. The filtrates were analyzed by ICP-OES.

3 RESULTS AND DISCUSSION

3.1 Fly ash physical and chemical properties

3.1.1 Elemental composition and mineralogy

The elemental composition of the original fly ash was determined by X-ray fluorescence spectroscopy. Si, Al and Ca were the major constituents of the original fly ash being 30.2%, 29.3% and 21.5% by weight (as SiO_2 , Al_2O_3 and CaO), respectively (Table 1). The high fraction of CaO indicated its potential for LFD treatment and CO_2 mineralization since CaO is the ideal feedstock for both chemical precipitation of LFD contaminants and CO_2 mineralization^[18]. Apart from CaO , the original fly ash sample contained various other alkaline and alkaline-earth elements, such as Mg, K and Na (3.16%, 0.7% and 0.4% by weight as MgO , K_2O and Na_2O , respectively). The results of elemental composition can help with phase peak identification in XRD analysis and results explanation of LFD treatment experiments.

Figure 3 shows a comparison of the XRD patterns of the unused and used fly ash samples for the four experiments. The unused fly ash (Fig. 3(a)) was mainly composed of various crystalline phases, including anhydrite (CaSO_4), calcite (CaCO_3), quartz (SiO_2), hematite (Fe_2O_3) and tricalcium aluminate ($\text{Ca}_3\text{Al}_2\text{O}_6$). Anhydrite and tricalcium aluminate were the dominating crystalline Ca-bearing phases. The broad background within 2–40 degrees of the XRD curve (Fig. 3(a)) indicated the presence of an amorphous phase in the unused fly ash^[30,31].

After experiment E1-P, the abundance of the amorphous phase did not change substantively (Fig. 3(b)). In addition, the peak intensity of calcite obviously increased while the peak intensities of anhydrite and tricalcium aluminate significantly decreased. This result can be explained by the CO_2 mineralization reaction between anhydrite and tricalcium aluminate and the CO_2 dissolved in the untreated LFD, which produced calcite^[32]. Similarly, the fly ash samples after experiments E2-PM and E4-PM also displayed significantly enhanced peak intensity of calcite and reduced anhydrite and tricalcium aluminate peaks (Fig. 3(c,e)). Also, the relative calcite peak intensity of fly ash in experiment E2-PM was much larger than that of fly ash in experiment E1-P. The reason for more calcite produced in experiment E2-PM might be more CO_2

available for mineralization reactions as CO_2 was bubbled into the suspension. In Fig. 3(d), calcite was the only phase identified in the used fly ash from experiment E3-PM.

3.1.2 Morphology

Figure 4 shows the SEM images of the unused and used fly ash samples for the four LFD treatments. The unused fly ash had irregular shaped particles (Fig. 4(a)). In the used fly ash, flocculent precipitation has formed on the external surfaces in E1-P (Fig. 4(b)). Compared to the unused samples, it was clear that the newly formed crystals had formed on the external surfaces of the particles or these had precipitated as separate fine particles (Fig. 4(c,d)). Most of the newly formed crystals (Fig. 4(c,d)) were cube-shaped and featured smooth surfaces, which was consistent with the typical calcite properties reported in the literature^[33]. This result provided direct evidence for the newly formed calcite phases shown in Fig. 3(c,e). More importantly, the newly formed calcite crystals featured smaller particle sizes (c. 1 μm) and more uniform cube shape (Fig. 4(c–f)), compared to those reported for a previous study^[34]. The reason for this might be the effect of organic species of the untreated LFD on the process of crystal formation. Earlier studies indicated that the nucleation rate of CaCO_3 was substantially affected by the difference in interfacial energy between crystal forms^[35]. The metastable morphology might tend to precipitate at high supersaturation of reactants. Organic molecules, such as humic and fulvic acids, could be adsorbed on the surface of the precipitated particles, therefore increasing the activated energy of the dissolved unstable precipitates and delaying the continuous transformation and growth of CaCO_3 to large calcite particles^[36].

3.2 Contaminant removal from liquid fraction of digestate by fly ash-based chemical precipitation and CO_2 mineralization

3.2.1 pH and electrical conductivity

The initial pH and EC of the untreated LFD were 8.3 units and 7.02 $\text{mS}\cdot\text{cm}^{-1}$, respectively (Table 1). In experiment E1-P, pH and EC of the treated LFD increased with the fly ash concentration (Fig. 5(a,b)). This phenomenon can be explained by the dissolution of metal oxides/hydroxides from the fly ash into the LFD during the experiment, which increased the concentrations of OH^- ions and metal ions^[18,37]. The fly ash sample contains various alkaline and alkaline-earth elements, such as Ca, Mg, Na, and K (21.5%, 3.16%, 0.4%, and 0.7% by weight as CaO , MgO , Na_2O , and K_2O , respectively) (Table 1). There was not any Na^+ and K^+ ions dissolved from fly ash into

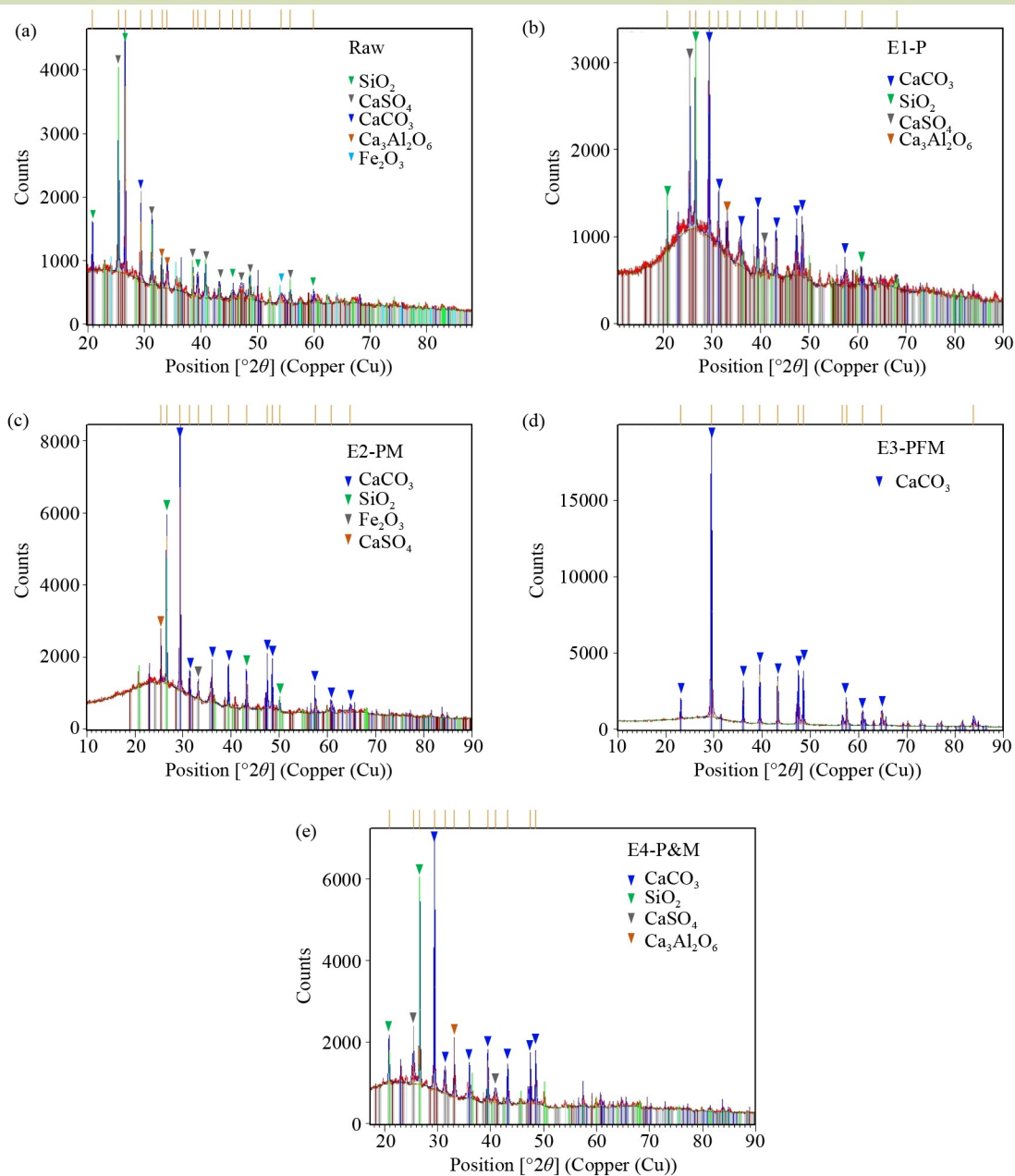


Fig. 3 X-ray diffraction patterns of the unused fly ash (a), and used fly ash from experiments E1-P (b), E2-PM (c), E3-PFM (d), and E4-P&M (e) with the fly ash at $200 \text{ g}\cdot\text{L}^{-1}$.

the LFD (Fig. 6(a,b)). The main ions that originated from fly ash into the LFD were Ca^{2+} and Mg^{2+} (Fig. 6(c,d)). The fly ash concentrations ranged from 25 to $200 \text{ g}\cdot\text{L}^{-1}$, and the highest pH and EC were obtained by the highest fly ash concentration ($200 \text{ g}\cdot\text{L}^{-1}$), which were 12.9 and $13.7 \text{ mS}\cdot\text{cm}^{-1}$ (Fig. 5(a,b)), respectively. Such results are expected since a larger fly ash concentration means more mineral components were dissolved in the treated LFD. For example, the Ca^{2+} concentration of the treated LFD increased from 124 to $1030 \text{ mg}\cdot\text{L}^{-1}$ as $200 \text{ g}\cdot\text{L}^{-1}$ of

fly ash was added to the untreated LFD (Fig. 6(c)).

In experiments E2-PM, E3-PFM and E4-P&M, the pH of the treated LFD decreased with CO_2 introduction into the treated LFD suspension (Fig. 5(a)). This observation is consistent with the neutral reaction between CO_2 and OH^- ions. In contrast, the changes in EC were more complex (Fig. 5(b)). The changes in EC in experiments E2-PM and E4-P&M were similar to those in experiment E1-P, where EC increased with fly ash

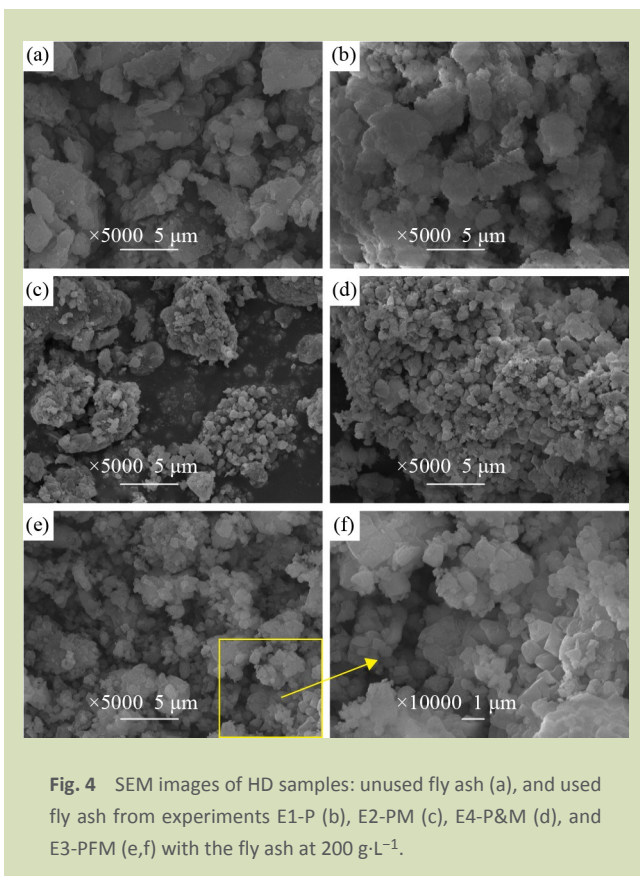


Fig. 4 SEM images of HD samples: unused fly ash (a), and used fly ash from experiments E1-P (b), E2-PM (c), E4-P&M (d), and E3-PFM (e,f) with the fly ash at 200 g·L⁻¹.

concentration even after CO₂ mineralization. This is reasonable given that more mineral components were removed by the dissolved CO₂ in experiments E2-PM and E4-P&M^[37]. This phenomenon is evidenced by the higher Ca²⁺ concentrations observed in experiments E2-PM and E4-P&M than in experiment E1-P (Fig. 6(c)). However, the EC in experiment E3-PFM decreased with fly ash concentration after CO₂ mineralization. This is likely to be due to the filtration treatment before CO₂ bubbling and there was no more mineral components removal during the CO₂ mineralization step. This finding can be confirmed by the lower Ca²⁺ and Mg²⁺ concentrations observed in experiment E3-PFM than that of experiments E2-PM and E4-P&M (Fig. 6(c,d)). The exhaust of metal ions and OH⁻ ions by CO₂ resulted in reduced EC. Overall, CO₂ bubbling after fly ash-based chemical precipitation helped neutralize the treated LFD and reduce the EC.

3.2.2 Chemical oxygen demand and total phosphate removal

The initial COD and TP of the untreated LFD were 817 and 21.5 mg·L⁻¹ (Table 1), respectively. In experiment E1-P, along with the fly ash concentration increased from 25 to 200 g·L⁻¹, the COD removal efficiencies increased from 26.3% to 93.8%

(Fig. 5(c)). The highest COD removal efficiencies were obtained with the highest fly ash concentration (200 g·L⁻¹). The COD removal can be explained by the removal of highly recalcitrant organic species, such as humic and fulvic acids^[26]. As fly ash was added to the untreated LFD, the partial dissolution of mineral components from the fly ash into the treated LFD contributed to an increased pH and concentration of polyvalent cations. The increased pH promoted the deprotonation of hydroxyl and carboxylic groups of the organic species, which facilitated the complexing of organic species with polyvalent cations and the subsequent precipitation^[26,28,29]. These results are consistent with earlier studies that used CaO as an agent for chemical precipitating^[18]. The XRD results (Fig. 3(a,b)) provide evidence for the presence of CaCO₃ in the used fly ash from experiment E1-P. The CaCO₃ might be produced by the reaction between the calcium-bearing phases of the fly ash and the initially dissolved CO₂ in the untreated LFD. Earlier studies indicated that organic species, such as humic and fulvic acids, could be co-precipitated with CaCO₃. Also, these organic species can also be adsorbed onto the surface of fly ash and CaCO₃ particles^[23,27]. Compared to experiment E1-P, higher COD removal efficiencies were achieved in experiments E2-PM, E3-PFM and E4-P&M at all fly ash concentrations. This can be explained by the CO₂ mineralization as CO₂ was introduced into the treated LFD suspension, which induced further precipitation. This finding is evidenced in XRD results (Fig. 3(c–e)), where the CaCO₃ peak intensities of fly ash samples from experiments E2-PM, E3-PFM and E4-P&M experiments were obviously larger than those from experiment E1-P.

TP was more sensitive to these chemical precipitation treatments than COD (Fig. 5(d)). Even with the lowest fly ash concentration (25 g·L⁻¹), the removal efficiencies of TP in the four experimental routes were higher than 80%. Along with the fly ash concentration increased from 25 to 200 g·L⁻¹, the TP removal efficiencies increased from 80% to 98%. Different treatments displayed very similar trends of TP removal. Considering that inorganic phosphorous was found to be dominant in the untreated LFD, which normally accounted for 60% to 80% of TP^[20], the removal of TP would be a combination mechanism of polyvalent cations and pH change induced by partial dissolution of fly ash components. Compared to the untreated LFD, the concentrations of Ca²⁺ and Mg²⁺ had increased significantly (Fig. 6(c,d)), indicating that the major contributors to TP precipitation were Ca²⁺ and Mg²⁺ dissolved from the fly ash. These results were consistent with earlier studies, in which the performance of Ca²⁺ and Mg²⁺ on inorganic phosphorus precipitation was

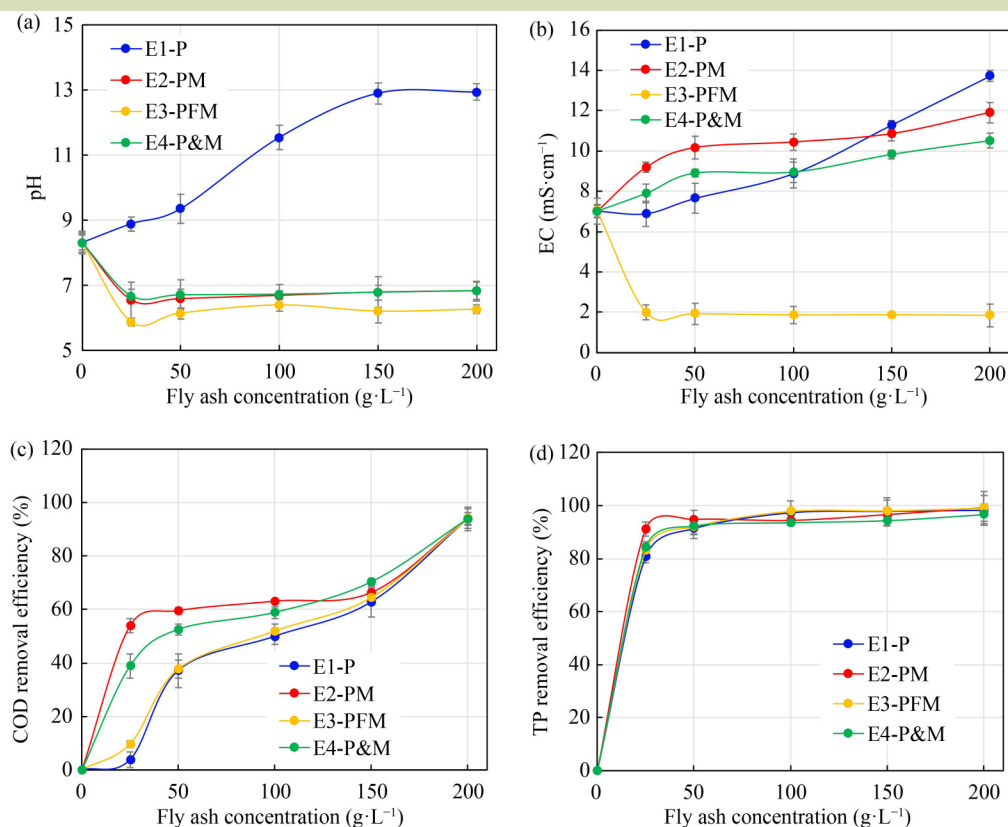


Fig. 5 Effect of various treatments on pH (a), electrical conductivity (EC) (b), chemical oxygen demand (COD) (c), and total phosphate (TP) (d) in treated liquid fraction of digestate over a range of concentrations.

investigated^[19,20]. In addition, earlier studies indicated that both Fe³⁺ addition and Mg²⁺ addition with pH adjustment gave comparable inorganic phosphorus removal efficiencies^[20]. However, Fe³⁺ concentrations in the treated LFD from the four experiments were lower than those in the untreated LFD (Fig. 6(e)). Also, the TP removal efficiency increased along with the increased pH (Fig. 5(a,d)), which is consistent with earlier studies that found that an acidic environment can slow down the precipitation reaction between Mg and phosphate, and the inorganic phosphorus removal efficiency by Mg²⁺ increased significantly as the pH was increased from about 7 to 9–13^[38–40]. Additionally, the removal of TP by Ca²⁺, Mg²⁺ and Fe³⁺ was normally precipitated as apatite, struvite and vivianite^[19,20]. However, none of these mineral phases were detected in the used fly ash samples (Fig. 3(c–e)). The reason for this might be the low TP concentration in the untreated LFD and the small amount of newly formed phosphorous-bearing precipitation.

Overall, fly ash performed well as a chemical precipitation agent for COD and TP removal from LFD. CO₂ bubbling after

fly ash-based chemical precipitation also provided further COD and TP removal by CO₂ mineralization of excessive alkaline mineral components in fly ash. Of the four treatment routes, the route for experiment E3-PFM is suggested as the best candidate given that it had > 93% COD and > 98% TP removal efficiencies and resulted in an EC of < 2 mS·cm⁻¹ EC and a neutral pH in the treated LFD. Considering the low price of fly ash, it can be used in high concentrations to achieve high COD and TP removal efficiencies without affecting the economic viability of the process. It has the potential to be used as an efficient, sustainable, and cost-effective alternative to the commonly applied chemical precipitation agent for LFD treatment.

3.2.3 Heavy metal removal

In experiment E1-P, adding fly ash to untreated LFD removed a substantial proportion of TP and organic contaminants that contributed to the COD, but there were still high concentrations of inorganic compounds, especially toxic metallic and nonmetallic ions in the treated LFD (Fig. 7). A portion of these toxic ions initially present in the LFD but some

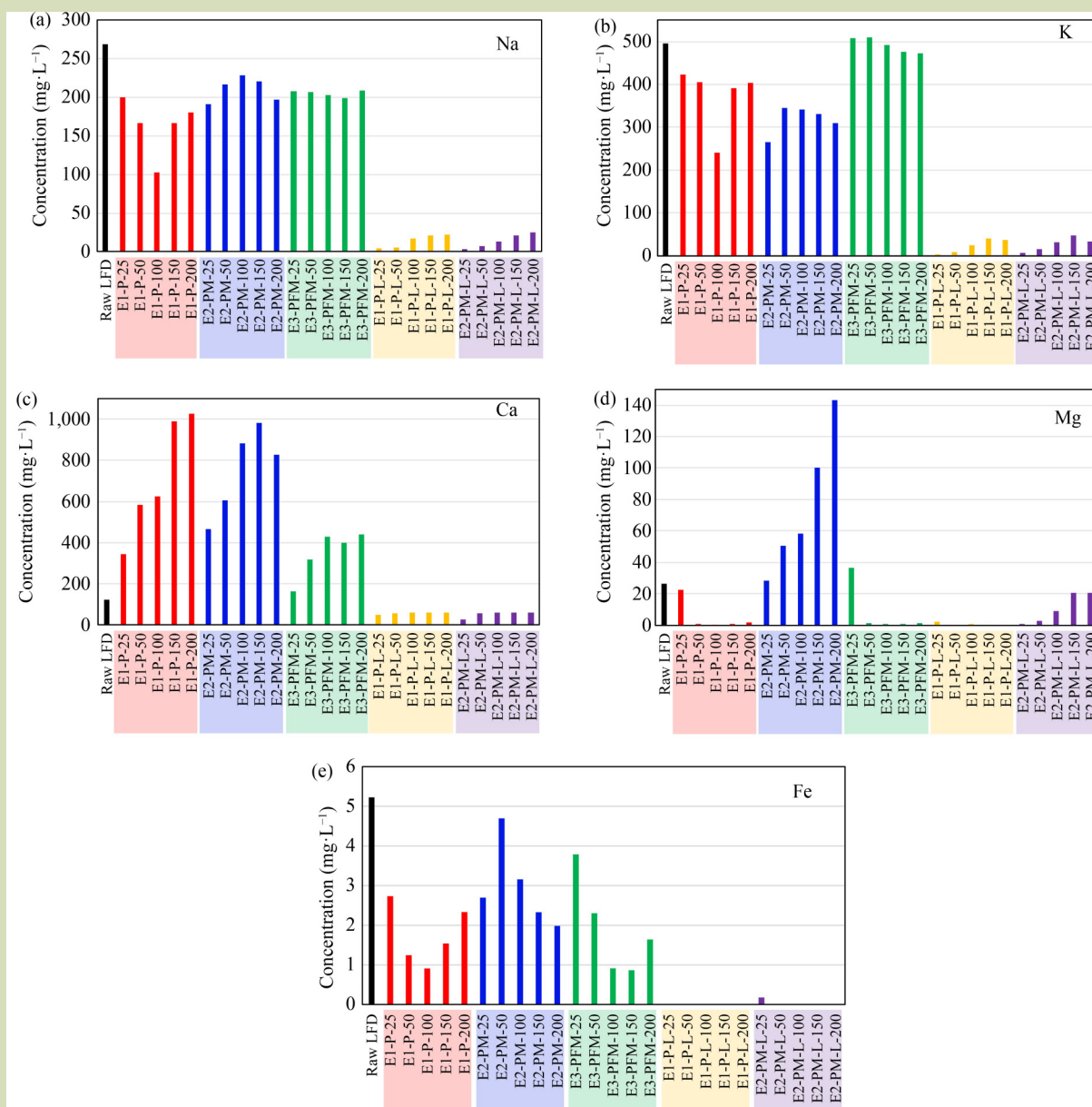


Fig. 6 Concentrations of major element ions Na (a), K (b), Ca (c), Mg (d), and Fe (e) in the treated liquid fraction of digestate (LFD) following four treatments.

were also be added with the fly ash. The initial concentrations of As, Cd, Cu, Cr, Mn, Ni, Pb, and Zn in the LFD were 0.588, 0.016, 0.534, 0.225, 0.275, 0.275, 0.281, and 2.95 mg·L⁻¹, respectively (Fig. 7). During the fly ash-based chemical precipitation process, there was a reaction balance between leaching from fly ash to the LFD and removal from LFD by precipitation for the toxic ions. After experiment E1-P by adding fly ash, different toxic ions had various changes in concentration. The concentrations of Cu, Mn, Ni, and Zn decreased with chemical precipitation, while the

concentrations of As, Cd, Cr, and Pb, increased. In experiment E2-PM, the introduction of CO₂ into the treated LFD suspension after fly ash-based chemical precipitation provided further removal of Cu, Cr, Mn, Ni, Pb, and Zn but not As and Cd. If route of experiment E3-PFM was used, the concentrations of toxic ions in the treated LFD significantly decreased, except for As, Cr, and Pb. Also, the leaching tests of used fly ash samples from experiments E1-P and E2-PM were performed by adding the untreated and treated samples into ultrapure water to evaluate the leaching characteristics of toxic

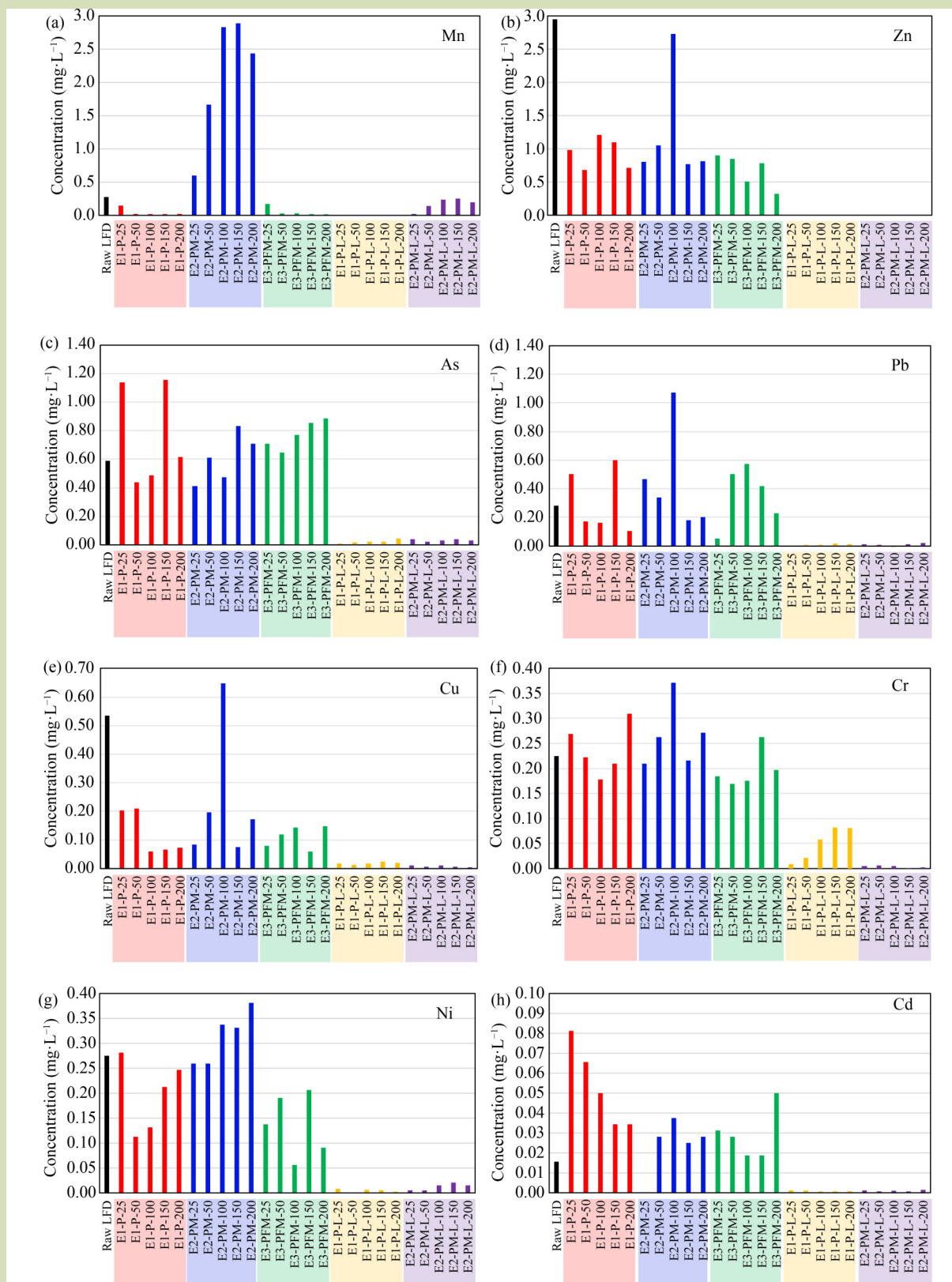


Fig. 7 Concentrations of microelement ions Mn (a), Zn (b), As (c), Pb (d), Cu (e), Cr (f), Ni (g), and Cd (h) in treated liquid fraction of digestate (LFD) following four treatments.

ions from the treated sample into the natural environment as the treated samples were disposed. Compared to the unused fly ash, the treated samples from experiments E1-P and E2PM released much lower concentrations of toxic ions, including As, Cd, Cu, Cr, Ni, Pb, and Zn (Fig. 7). This phenomenon might result from the co-precipitation of COD, TP, CaO, and CO₂ (Fig. 4(b-d)). Newly formed flocculent precipitation and cube shape calcite crystals grew on the external surface of the fly ash particles, which inhibited further removal of toxic ions. To summarize, compared to experiment E1-P, the routes of experiments E2-PM, E3-PFM, and E4-P&M not only provided further COD and TP removal but also removal of some toxic ions, especially the heavy metals.

4 CONCLUSIONS

Chemical precipitation is a widely applied approach for an LFD but its large-scale application requires low-cost and efficient precipitating agents and novel process design. This study evaluated a novel approach for the efficient removal of contaminants from the LFD by fly ash-based chemical precipitation, followed by filtration and CO₂ mineralization. Technical feasibility of this approach was evaluated by changes

in pH and EC, and removal efficiencies of TP, COD and heavy metals during the treatment. The fly ash used in this study performed well as a chemical precipitation agent for COD and TP removal from LFD. CO₂ bubbling after fly ash-based chemical precipitation also provided further COD and TP removal by CO₂ mineralization of excessive alkaline mineral components in fly ash. The removal of COD and TP was achieved by the co-precipitation of these contaminants with CaCO₃. Although adding fly ash to LFD increased pH and EC, CO₂ bubbling after fly ash-based chemical precipitation helped neutralize the treated LFD and reduced the EC, as well as the removal of some toxic ions, especially the heavy metals. During experiment E3-PFM, calcite crystals with small particle sizes (c. 1 μm) and uniform cube shapes were obtained asserted by the effect of organic species of LFD on the process of crystal growth. Of the four treatment routes, the route of experiment E3-PFM is suggested as the best candidate given that it had > 93% COD and > 98% TP removal efficiencies, and resulted in an EC of < 2 mS-cm⁻¹ and a neutral pH in the treated LFD, as well as calcite product. The treated LFD can meet the requirement for irrigation water. Considering the low price of fly ash, it can be used in high concentrations to achieve high COD and TP removal efficiencies without harming the economic feasibility of the process.

Acknowledgements

The authors thank the financial supports from the Jinhua Polytechnic (SGYC11070201X004), Jinhua City Public Welfare Application Research Project (2022-4-002), and Fundamental Research Funds for the Central Universities (2662020GXD002).

Compliance with ethics guidelines

Zhengxin Fei, Zijie Ding, Xuan Zheng, Liang Feng, Qingyao He, Shuiping Yan, and Long Ji declare that they have no conflicts of interest or financial conflicts to disclose. This article does not contain any studies with human or animal subjects performed by any of the authors.

REFERENCES

1. Lü F, Wang Z, Zhang H, Shao L, He P. Anaerobic digestion of organic waste: recovery of value-added and inhibitory compounds from liquid fraction of digestate. *Bioresource Technology*, 2021, **333**: 125196
2. Guo X, Cui X, Li H. Effects of fillers combined with biosorbents on nutrient and heavy metal removal from biogas slurry in constructed wetlands. *Science of the Total Environment*, 2020, **703**: 134788
3. Zeng W, Wang D, Wu Z, He L, Luo Z, Yang J. Recovery of nitrogen and phosphorus fertilizer from pig farm biogas slurry and incinerated chicken manure fly ash. *Science of the Total Environment*, 2021, **782**: 146856
4. Liang F, Xu L, Ji L, He Q, Wu L, Yan S. A new approach for biogas slurry disposal by adopting CO₂-rich biogas slurry as the flower fertilizer of *Spathiphyllum*: feasibility, cost and environmental pollution potential. *Science of the Total Environment*, 2021, **770**: 145333
5. Alengebawy A, Jin K, Ran Y, Peng J, Zhang X, Ai P. Advanced pre-treatment of stripped biogas slurry by polyaluminum chloride coagulation and biochar adsorption coupled with ceramic membrane filtration. *Chemosphere*, 2021, **267**: 129197
6. Shi M, He Q, Feng L, Wu L, Yan S. Techno-economic evaluation of ammonia recovery from biogas slurry by vacuum membrane distillation without pH adjustment. *Journal of*

- Cleaner Production*, 2020, **265**: 121806
7. Moure Abelenda A, Semple K T, Lag-Brotons A J, Herbert B M J, Aggidis G, Aiouache F. Kinetic study of the stabilization of an agro-industrial digestate by adding wood bottom ash. *Chemical Engineering Journal Advances*, 2021, **7**: 100127
 8. Petrovič A, Simonič M, Čuček L. Nutrient recovery from the digestate obtained by rumen fluid enhanced anaerobic co-digestion of sewage sludge and cattail: Precipitation by $MgCl_2$ and ion exchange using zeolite. *Journal of Environmental Management*, 2021, **290**: 112593
 9. Ansari F A, Nasr M, Rawat I, Bux F. Meeting sustainable development goals (SDGs) through progression of pilot-scale algal system to commercial raceway pond (300,000 L). *Biomass Conversion and Biorefinery*, 2021 doi: [10.1007/s13399-021-01661-0](https://doi.org/10.1007/s13399-021-01661-0)
 10. Palakodeti A, Azman S, Rossi B, Dewil R, Appels L. A critical review of ammonia recovery from anaerobic digestate of organic wastes via stripping. *Renewable & Sustainable Energy Reviews*, 2021, **143**: 110903
 11. Drapanauskaite D, Handler R M, Fox N, Baltrusaitis J. Transformation of liquid digestate from the solid-separated biogas digestion reactor effluent into a solid NH_4HCO_3 fertilizer: sustainable process engineering and life cycle assessment. *ACS Sustainable Chemistry & Engineering*, 2021, **9**(1): 580–588
 12. Chen X, Wendell K, Zhu J, Li J, Yu X, Zhang Z. Synthesis of nano-zeolite from coal fly ash and its potential for nutrient sequestration from anaerobically digested swine wastewater. *Bioresource Technology*, 2012, **110**: 79–85
 13. Li J, Zhang Z, Khunjar W, Zhao K. Enhanced nutrient sequestration from swine wastewater using zeolite synthesized from fly ash integrated with surface amendment technique. *Fuel*, 2013, **111**: 57–65
 14. Wang P, Zhang X, Gouda S G, Yuan Q. Humidification-dehumidification process used for the concentration and nutrient recovery of biogas slurry. *Journal of Cleaner Production*, 2020, **247**: 119142
 15. Fernandes F, Silkina A, Fuentes-Grünwald C, Wood E E, Ndovela V L S, Oatley-Radcliffe D L, Lovitt R W, Llewellyn C A. Valorising nutrient-rich digestate: dilution, settlement and membrane filtration processing for optimisation as a waste-based media for microalgal cultivation. *Waste Management*, 2020, **118**: 197–208
 16. Ahmad Ansari F, Nasr M, Guldhe A, Kumar Gupta S, Rawat I, Bux F. Techno-economic feasibility of algal aquaculture via fish and biodiesel production pathways: a commercial-scale application. *Science of the Total Environment*, 2020, **704**: 135259
 17. Kumar Gupta S, Kumar N M, Guldhe A, Ahmad Ansari F, Rawat I, Nasr M, Bux F. Wastewater to biofuels: comprehensive evaluation of various flocculants on biochemical composition and yield of microalgae. *Ecological Engineering*, 2018, **117**: 62–68
 18. Viegas C, Nobre C, Mota A, Vilarinho C, Gouveia L, Gonçalves M. A circular approach for landfill leachate treatment: chemical precipitation with biomass ash followed by bioremediation through microalgae. *Journal of Environmental Chemical Engineering*, 2021, **9**(3): 105187
 19. Cao X, Harris W. Carbonate and magnesium interactive effect on calcium phosphate precipitation. *Environmental Science & Technology*, 2008, **42**(2): 436–442
 20. Li L, Pang H, He J, Zhang J. Characterization of phosphorus species distribution in waste activated sludge after anaerobic digestion and chemical precipitation with Fe^{3+} and Mg^{2+} . *Chemical Engineering Journal*, 2019, **373**: 1279–1285
 21. Harris D, Heidrich C, Feuerborn J. Global aspects on coal combustion products. In: Proceedings of the world of coal ash (WOCA), St. Louis, MO, USA, 2019, 13–16
 22. Yao Z T, Ji X S, Sarker P K, Tang J H, Ge L Q, Xia M S, Xi Y Q. A comprehensive review on the applications of coal fly ash. *Earth-Science Reviews*, 2015, **141**: 105–121
 23. Sanna A, Uibu M, Caramanna G, Kuusik R, Maroto-Valer M M. A review of mineral carbonation technologies to sequester CO_2 . *Chemical Society Reviews*, 2014, **43**(23): 8049–8080
 24. Deonaraine A, Lau B L T, Aiken G R, Ryan J N, Hsu-Kim H. Effects of humic substances on precipitation and aggregation of zinc sulfide nanoparticles. *Environmental Science & Technology*, 2011, **45**(8): 3217–3223
 25. Zhai H, Wang L, Hövelmann J, Qin L, Zhang W, Putnis C V. Humic acids limit the precipitation of cadmium and arsenate at the brushite-fluid interface. *Environmental Science & Technology*, 2019, **53**(1): 194–202
 26. Zheng L, Pan Y, Zhao Y G. Biomineralization eliminating marine organic colloids (MOCs) during seawater desalination: mechanism and efficiency. *Biochemical Engineering Journal*, 2020, **161**: 107705
 27. Wang H, Alfredsson V, Tropsch J, Ettl R, Nylander T. Effect of polyelectrolyte and fatty acid soap on the formation of $CaCO_3$ in the bulk and the deposit on hard surfaces. *ACS Applied Materials & Interfaces*, 2015, **7**(38): 21115–21129
 28. Phillips B L, Lee Y J, Reeder R J. Organic coprecipitates with calcite: NMR spectroscopic evidence. *Environmental Science & Technology*, 2005, **39**(12): 4533–4539
 29. Loste E, Díaz-Martí E, Zarbakhsh A, Meldrum F C. Study of calcium carbonate precipitation under a series of fatty acid Langmuir monolayers using Brewster angle microscopy. *Langmuir*, 2003, **19**(7): 2830–2837
 30. Ji L, Yu H, Wang X, Grigore M, French D, Gözükar Y M, Yu J, Zeng M. CO_2 sequestration by direct mineralisation using fly ash from Chinese Shenfu coal. *Fuel Processing Technology*, 2017, **156**: 429–437
 31. Ji L, Yu H, Yu B, Zhang R, French D, Grigore M, Wang X, Chen Z, Zhao S. Insights into carbonation kinetics of fly ash from victorian lignite for CO_2 sequestration. *Energy & Fuels*, 2018, **32**(4): 4569–4578
 32. Ji L, Yu H, Zhang R, French D, Grigore M, Yu B, Wang X, Yu J, Zhao S. Effects of fly ash properties on carbonation efficiency in CO_2 mineralisation. *Fuel Processing Technology*, 2019, **188**:

- 79–88
33. Hong S, Sim G, Moon S, Park Y. Low-temperature regeneration of amines integrated with production of structure-controlled calcium carbonates for combined CO₂ capture and utilization. *Energy & Fuels*, 2020, **34**(3): 3532–3539
 34. Zheng X, Zhang L, Feng L, He Q, Ji L, Yan S. Insights into dual functions of amino acid salts as CO₂ carriers and CaCO₃ regulators for integrated CO₂ absorption and mineralization. *Journal of CO₂ Utilization*, 2021, **48**: 101531
 35. Cantaert B, Kim Y Y, Ludwig H, Nudelman F, Sommerdijk N A J M, Meldrum F C. Think positive: phase separation enables a positively charged additive to induce dramatic changes in calcium carbonate morphology. *Advanced Functional Materials*, 2012, **22**(5): 907–915
 36. Addadi L, Raz S, Weiner S. Taking advantage of disorder: amorphous calcium carbonate and its roles in biomineralization. *Advanced Materials*, 2003, **15**(12): 959–970
 37. Kang J M, Murnandari A, Youn M H, Lee W, Park K T, Kim Y E, Kim H J, Kang S P, Lee J H, Jeong S K. Energy-efficient chemical regeneration of AMP using calcium hydroxide for operating carbon dioxide capture process. *Chemical Engineering Journal*, 2018, **335**: 338–344
 38. Li H, Yao Q Z, Dong Z M, Zhao T L, Zhou G T, Fu S Q. Controlled synthesis of struvite nanowires in synthetic wastewater. *ACS Sustainable Chemistry & Engineering*, 2019, **7**(2): 2035–2043
 39. Perwitasari D S, Muryanto S, Jamari J, Bayuseno A P. Kinetics and morphology analysis of struvite precipitated from aqueous solution under the influence of heavy metals: Cu²⁺, Pb²⁺, Zn²⁺. *Journal of Environmental Chemical Engineering*, 2018, **6**(1): 37–43
 40. Le V G, Vu C T, Shih Y J, Bui X T, Liao C H, Huang Y H. Phosphorus and potassium recovery from human urine using a fluidized bed homogeneous crystallization (FBHC) process. *Chemical Engineering Journal*, 2020, **384**: 123282